Optical and electrophysical properties of nanocomposites based on PEDOT: PSS and gold/silver nanoparticles

7 authors, including:

Alexander Kukhta
Belarusian State University
125 PUBLICATIONS **525** CITATIONS

Artyom Pochtenny
Belarusian State Technological University
14 PUBLICATIONS **35** CITATIONS

Aliaksei Vasilievich Misevich
19 PUBLICATIONS **67** CITATIONS

Vorobyova Svetlana
Research Institute for Physical Chemical Problems
41 PUBLICATIONS **359** CITATIONS

Some of the authors of this publication are also working on these related projects:

Project   Conducting, magnetic and luminescent polymer-graphene based triple composites View project

SURFACE PHYSICS
AND THIN FILMS

Optical and Electrophysical Properties of Nanocomposites Based on PEDOT : PSS and Gold/Silver Nanoparticles

A. V. Kukhta[a], *, A. E. Pochtenny[b], A. V. Misevich[b], I. N. Kukhta[c], E. M. Semenova[d], S. A. Vorobyova[d], and E. Sarantopoulou[e]

[a] Research Institute of Nuclear Problems, Belarusian State University, ul. Bobruiskaya 11, Minsk 220030 Belarus

* e-mail: al.kukhta@gmail.com

[b] Belarusian State Technological University, ul. Sverdlova 13a, Minsk, 220006 Belarus

[c] Institute of Chemistry of New Materials, National Academy of Sciences of Belarus, ul. F. Skoriny 36, Minsk, 220141 Belarus

[d] Research Institute of Physics-Chemistry Problems, Belarusian State University, ul. Leningradskaya 14, Minsk, 220030 Belarus

[e] Theoretical and Physical Chemistry Institute, National Hellenic Research Foundation, 48 Vasileos Constantinou Avenue, Athens, 11635 Greece

Received September 30, 2013

Abstract—The absorption spectra in the visible region and current–voltage characteristics in a wide range of electric fields have been investigated at the macroscopic level (planar structures) and at the microscopic level (using a conductive atomic force microscope) in films based on the electroactive polymer PEDOT : PSS and gold/silver nanoparticles (PEDOT : PSS + Au/AgNP). It has been shown that the behavior of the current–voltage characteristics of the nanocomposite films depends significantly on the electric field strength. It has been found that the introduction of gold nanoparticles into PEDOT : PSS in weak electric fields leads to an increase in the bulk conductance by almost two orders of magnitude (due to donor–acceptor interactions), a 50% decrease in the conduction activation energy, and an increase in the sensitivity to adsorbed oxygen. It has been demonstrated that electrical conduction of PEDOT : PSS + AuNP films is provided by hopping charge transfer both in the system of intrinsic localized states and in the system of impurity states of adsorbed oxygen. In strong electric fields, the current–voltage characteristics exhibit a different behavior in the forward and reverse scanning modes.

DOI: 10.1134/S1063783414040131

1. INTRODUCTION

Owing to their unique properties, electroactive conjugated polymers are of great interest as electronic materials [1]. Products of these materials can be easily made into desired shapes; moreover, they possess flexibility and are significantly lighter than metal products. However, polymers have a lower electrical conductivity as compared to metals and are less stable, especially under ultraviolet irradiation. Temperature and other environmental parameters can substantially affect the functional characteristics of the polymers. These disadvantages present considerable difficulties for their practical application. One possible way to overcome these difficulties is the formation of composite metal–polymer structures, in particular, the introduction of noble metal nanoparticles into a polymer matrix. Such nanocomposites, for example, can serve as the basis for non-volatile memory elements with two stable states, namely, a high-conductance state and a low-conductance state, the switching between which occurs through the change in the level of applied voltage [2, 3]. Furthermore, these nano-

composites provide the basis for the development of electrically conductive electrodes that are intended for electronic devices [4] and suitable for deposition by the supercheap printing method. Metal nanoparticles are introduced into active media of electronic devices [5].

As a rule, the electrical conductance of a composite based on conductive particles dispersed in a dielectric matrix critically depends on the concentration of the conductive component and can be described by the classical percolation theory [6]. According to this theory, the composite abruptly becomes conductive at a concentration of the conducting phase above the percolation threshold, at which the conductive component of the composite forms an infinite cluster. In the case of a semiconductor matrix (for example, a polymer with conjugated bonds), metal nanoparticles dispersed in this matrix can affect the conductance of the composite at concentrations considerably below the percolation threshold. The electrical impedance of a polymer nanocomposite can be represented as the sum of the resistances of polymer moieties, nanoparticles, and boundaries between the polymer and the nanoparticles. Owing to changes in the properties of these

boundaries, the electrical conductance of polymer nanocomposites was greatly improved [7−10]. The electrical conductance of composites based on conjugated polymers containing metal nanoparticles has been repeatedly studied (see, for example, [11−15]); however, the mechanism of this conduction remains controversial.

This work is devoted to the study of some optical and electrophysical properties of nanocomposites in which the semiconducting matrix is a mixture of polyethylenedioxythiophene (PEDOT) with polystyrene sulfonate (PSS), namely, PEDOT : PSS, and silver or gold nanoparticles serve as the filler. The polymer PEDOT : PSS is one of the most promising materials for organic electronics due to the high chemical and thermal stability, transparency in the visible spectral range, and possibility of synthesizing films based on it from aqueous solutions [16, 17]. PEDOT : PSS is used as a layer injecting holes, both in electroluminescent [18] and photovoltaic [19] devices, memory elements [2], resistive switches [20, 21], etc. The introduction of metal nanoparticles, actively injecting electrons, into a polymer matrix makes it possible to fabricate nanostructures with an increased conductance, which is the practical purpose of our work. Moreover, the purpose of the investigation of the optical and electrophysical properties is to elucidate some aspects of the mechanism of electrical conduction in polymers and related nanocomposite structures. Nanoparticles of gold (AuNP) and silver (AgNP) are characterized by ease of preparation, stability, and good plasmonic properties.

## 2. SAMPLE PREPARATION AND EXPERIMENTAL TECHNIQUE

Gold colloidal solutions stabilized by sodium folate were prepared by the reduction of $HAuCl_4 \cdot H_2O$ with sodium borohydride in the presence of sodium folate as a stabilizer [22] at the initial ratio $HAuCl_4 : NaBH_4 :$ sodium folate = 1 : 4 : 0.25. The concentration of the gold hydrosol was 0.75×10^{-3} M. Silver colloidal solutions were prepared by the reduction of $AgNO_3$ with sodium borohydride upon addition of sodium oleate [23]. PEDOT : PSS (low conductance) was purchased from Aldrich and used without purification.

The synthesis of homogeneous and reproducible samples of the "metal nanoparticle metal/conductive polymer" nanocomposites is a nontrivial but fairly simple process. A colloidal solution containing PEDOT : PSS and nanoparticles of Au or Ag was prepared by mixing of aqueous solutions and ultrasonic treatment for 15 min. Thin films of the polymer or the nanocomposite were prepared by centrifugation of the corresponding solution on a polycor substrate with an interdigitated system of Ni electrodes separated by a distance of 100−110 μm (for electrophysical measurements), on a quartz substrate (for optical measurements), or on a silicon substrate (for conductance

measurements using a conductive atomic force microscope (C-AFM)), followed by heating under vacuum at a temperature of 100°C for 30 min. The film thickness was 60−80 nm. Before deposition, the substrates were ultrasonically cleaned in organic solvents for 15 min, dried in a nitrogen flow, and then irradiated with oxygen plasma for 15 min.

The electrical conductance G and temperature dependence of the electrical conductance measured for thin films on substrates with an interdigitated system of Ni electrodes under vacuum with a residual pressure of 10^{-2} Pa were investigated using measurements of current−voltage characteristics and cyclic thermal desorption [24, 25]. The cyclic thermal desorption method is based on the fact that the conductance of the majority of organic films depends on the concentration of adsorbed oxygen molecules, which can decrease during heating of the sample. Upon heating of the sample under vacuum to a particular temperature, the concentration of adsorbed oxygen in the sample reaches a specific controlled value. By cooling the sample under vacuum from this temperature, we can measure the temperature dependence of the conductance at a constant concentration of adsorbed oxygen in the sample. Thus, the successive heating of the sample to increasingly higher temperatures and the subsequent measurement of the temperature dependences of the electrical conductance during cooling from these temperatures under vacuum make it possible to obtain a set of temperature dependences of the conductance for different concentrations of adsorbed oxygen in the same sample. After these measurements, we calculated the electrical conductance G (at a temperature of 300 K), which is related to the initial value G_0 (or the pre-exponential factor determining the probability of nonresonant tunneling of electrons between neighboring localization centers providing the hopping conduction mechanism) and the activation energy E_a by the formula $G = G_0 \exp(-E_a/kT)$, where k is the Boltzmann constant. The maximum heating temperature T was 124°C.

The other electrical measurements were performed using a Veeco Innova atomic force microscope in the conductive mode (C-AFM). The instrument was placed in a noise insulation box on a vibration quenching substrate at room-temperature conditions. The probe used for C-AFM measurements was coated by a Pt/Ir layer. The Pt/Ir coating provided metallic conductivity of the probe holder and increased the durability of the film. The tip radius was 20 nm, the typical elastic constant was 0.2 N/m, and the resonance frequency was 13 kHz. Before measurements, the C-AFM signal was tested with the reference sample. The studied sample was fixed on a metal holder with silver paste. The metal holder was kept positively charged. The probe was placed at the chosen point on the surface, and the applied voltage was varied from −8 to 8 V
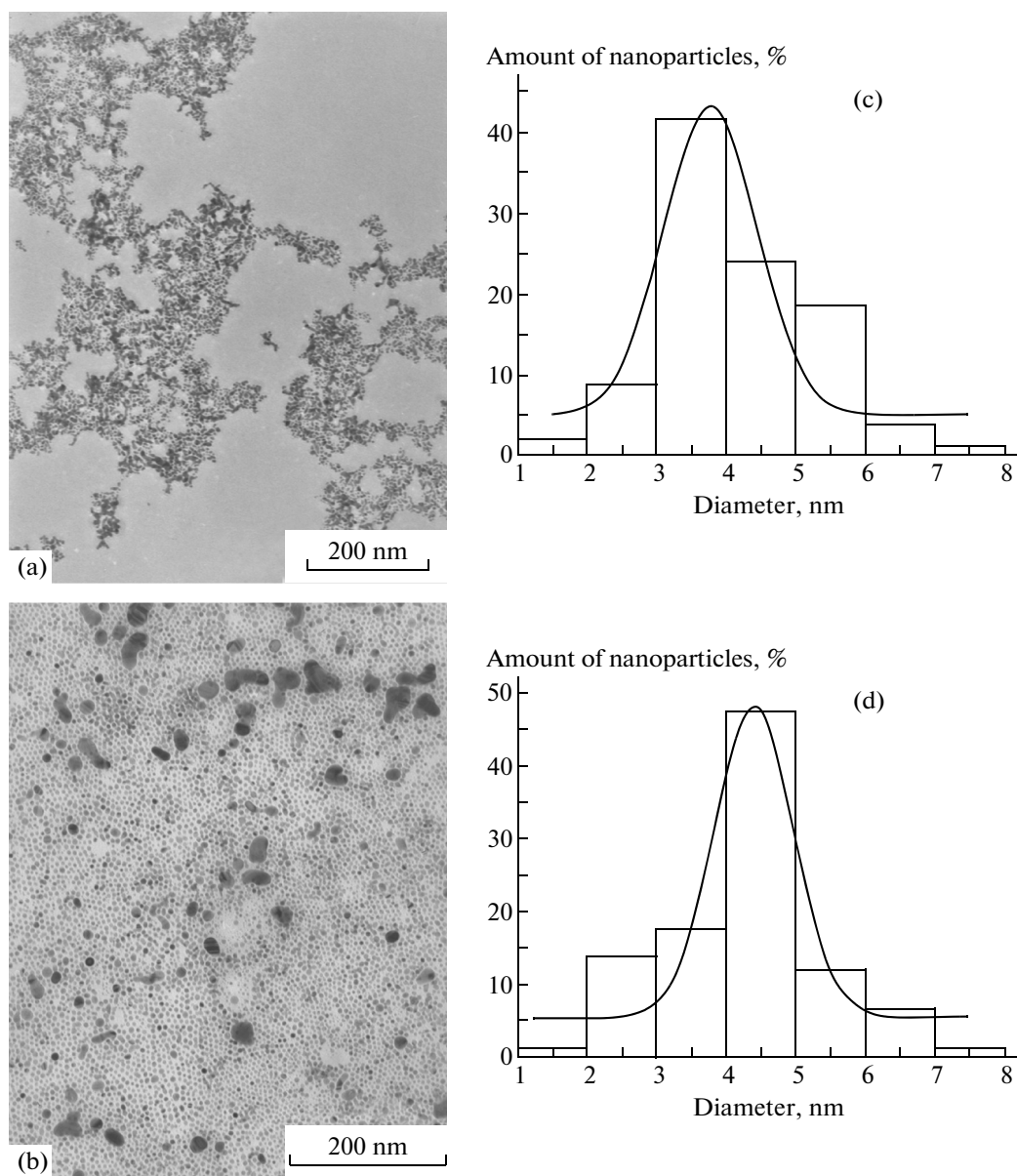
Fig. 1. (a, c) Micrographs and (b, d) size distributions of nanoparticle in the dispersed phase of (a, b) Au and (c, d) Ag hydrosols.

for a few seconds. Silver nanoparticles were chosen as the material with the highest plasmon effect [26].

The optical absorption spectra were recorded on a Cary 500 Scan UV–VIS–NIR spectrophotometer (Varian Ltd.). The size of particles and the composition of the dispersed phase were examined using a LEO-906 transmission electron microscope with a resolution of 0.1 nm at 100 kV.

3. RESULTS AND DISCUSSION

The images obtained using a transmission electron microscope and the size distributions of Au and Ag nanoparticles in a colloidal dispersion are shown in Fig. 1. According to the electron microscopy data, the

Au nanoparticles have a predominantly spherical shape with an average diameter of 3.78 nm and a root-mean-square deviation of 0.19 nm. This sample is characterized by sedimentation stability, which is confirmed by its optical characteristics (not presented here). A small absorption maximum is observed at 545 nm (Fig. 2, curve *1*), which confirms the electron microscopy data presented above. The height of the absorption maximum does not change with time. The Ag nanoparticles with an average diameter of 4.9 nm and a root-mean-square deviation of 0.11 nm are distributed more uniformly. The absorption maximum of the colloid in the region of 420 nm (curve *4*) is also consistent with the electron microscopy data. The absorption spectrum of the nanocomposite film

Optical density, arb. units
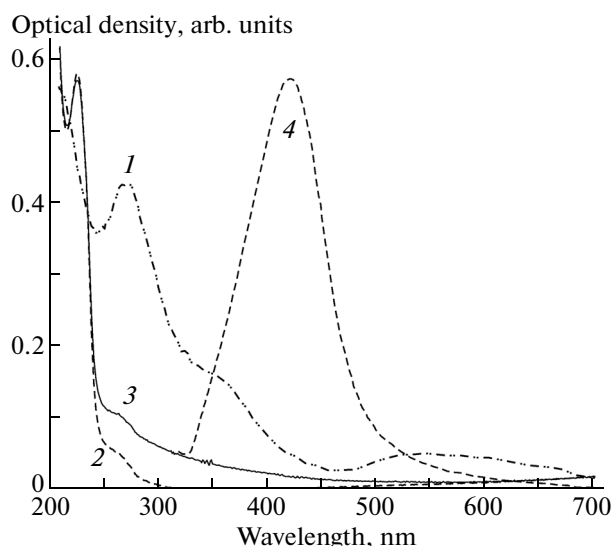
Fig. 2. Absorption spectra of (*1*) aqueous gold colloid (1.75×10^{-3} M) stabilized by sodium folate, (*2*) PEDOT : PSS thin film, (*3*) PEDOT : PSS + AuNP thin film, and (*4*) aqueous silver colloid.

(curve *3*) in the short-wavelength region is slightly changed compared with the spectrum of the pure polymer film (curve *2*). The nanocomposite films remain transparent over the entire visible spectral range (the decrease in transparency does not exceed 3%). A noticeable absorption is observed only at wavelengths less than 400 nm.

The AFM measurements did not reveal significant differences in the morphologies of thin films of the pure PEDOT : PSS and the polymer containing nanoparticles. However, at low applied voltages, for both films there is no noticeable correlation between the morphology and the electric current distribution (Fig. 3), although a certain correlation appears as the voltage increases. Furthermore, the currents of PEDOT : PSS + AgNP films are larger in magnitude and have a more pronounced structure than those of the pure polymer films. This means that the nanoparticles are located under the film surface at different distances from it and initiate an increase in the current. The electric field strength in this geometry is difficult to estimate. Based on the ratio of the voltage to the interelectrode distance, it exceeds 1000 kV/cm. The sharp electrode further increases the voltage. Therefore, these measurements can be considered as measurements in a very strong electric field. The observed current–voltage characteristics (Fig. 4) are nonlinear for both the pure PEDOT : PSS and composite PEDOT : PSS + AgNP films. This nonlinearity can arise from the point contact that is formed by the conductive probe and has the character of Schottky barrier, which should be taken into account. The current–voltage curves for the pure film PEDOT : PSS have a plateau between −2 and 2 V and coincide for the

forward and reverse scanning modes (Fig. 4a). In the case of the nanocomposite film (Fig. 4b), the curves are characterized both by a continuous nonlinear increase in the current up to a specific value, at which the surface and the tip are destroyed, and by a difference in their behavior in the forward (solid line) and reverse (dashed line) scanning modes at voltages ranging between −8 and 8 V. The curves measured at different points of the film have a similar behavior with several varying bias potentials. This bistable behavior of the current–voltage characteristic can be explained by strong-electric-field-induced charge transfer from the electron-donating polymer molecules to the electron-acceptor metal nanoparticles. In the nanocomposite films, there is also an increase in the local electric field induced by nanoparticles in an external field [26], which leads to an enhancement in the charge-transfer transitions and, accordingly, the charge transport and the flowing current.

The current–voltage characteristics of planar thin films of the pure polymer and the nanocomposite with gold nanoparticles are shown in Fig. 5. It should be noted that, in structures with an interdigitated system of electrodes, there arises a good symmetric contact, and the absence of contact problems with nickel electrodes was checked by test measurements for phthalocyanine with the known electrophysical characteristics. Initially, the measurements were carried out with variations in the voltage in the range from 0 to 10 V. Taking into account the interelectrode distance, we can assume that these measurements were performed in the mode of weak fields. It can be seen that the current in the nanocomposite film is approximately two orders of magnitude higher than that in the pure polymer film, which is in agreement with the data reported in [12]. In the voltage range under consideration, this dependence is linear and completely reversible for a large number of forward and reverse runs; i.e., in weak fields, this material is electrically stable. If the voltage of the first scanning exceeds 50 V, the current decreases. In the reverse scanning mode, the current decreases, but slightly exceeds the corresponding currents for the pure polymer. In the second and third scannings, the increase in the current is less pronounced, and the difference in the curves for the forward and reverse scanning modes decreases. This behavior of the current–voltage characteristics is opposite to that observed in nanocomposite memory devices [2], in which the current during the first scanning is considerably less than that during the subsequent scannings. An extensive literature on organic memory devices with nanoparticles was reviewed in detail in [2, 27, 28], where it was determined that the main mechanisms of the process can be as follows: (1) electric-field-induced charge transfer between the nanoparticles and the surrounding conjugated compounds; (2) conduction through filaments formed by nanoparticles due to the electrophoresis; (3) trapping/release of charge carriers; and (4) inhibition of
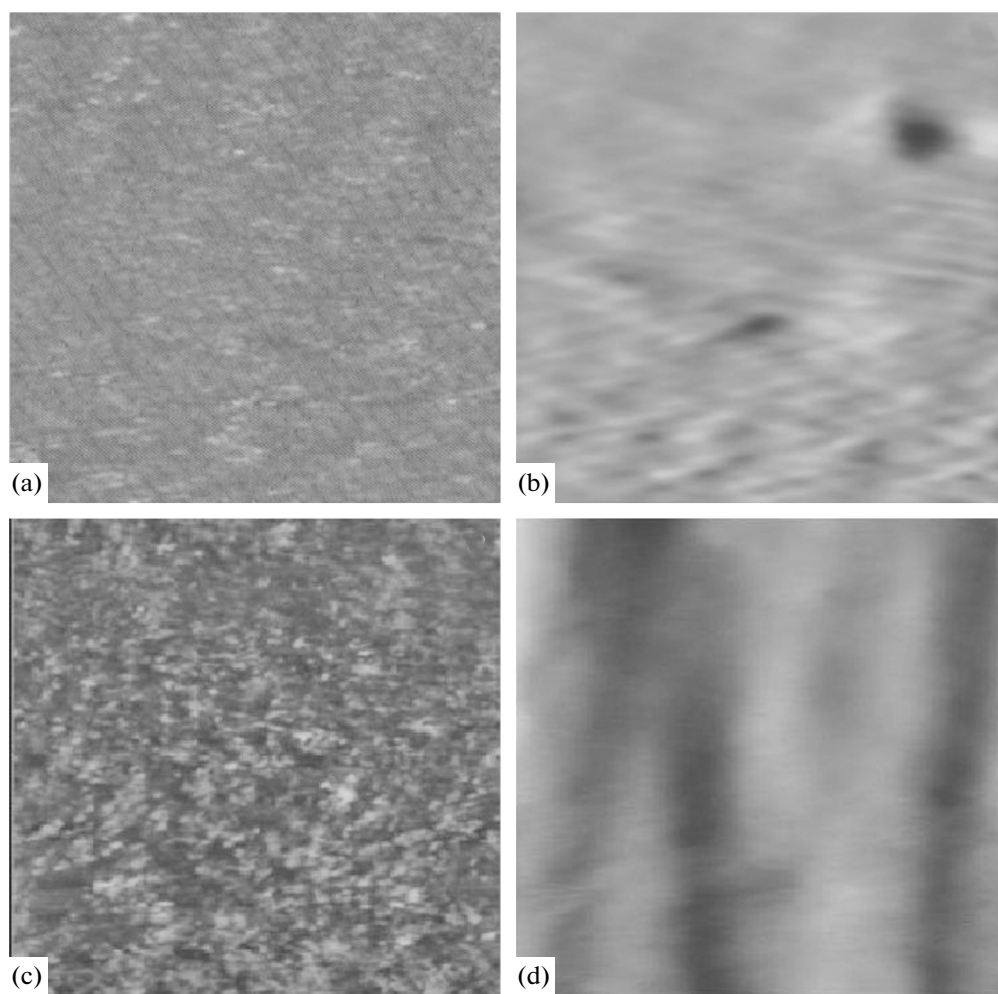
Fig. 3. (a, c) Electric current distributions and (b, d) topographies of (a, b) PEDOT : PSS and (c, d) PEDOT : PSS + AgNP films (1 × 1 μm in size) at a positive potential of 0.3 V across the sample.

injection from nanoparticles by the space-charge field. The mechanism of the memory effect is often assigned to the electrically induced charge transfer between the nanoparticles, which leads to a drastic change in the electrical conductance of organic thin films [29]. It should be noted that the planar structure considered by us differs from the memory devices presented in the literature by the interelectrode distance, which, in our case, is three orders of magnitude larger. The applied electric field in our structure (~5 kV/cm at 10 V) is at least one order of magnitude smaller than that in the aforementioned memory devices. Typical transitions to a high-conductance state are induced by an electric field ranging from 60 to 100 kV/cm [2, 27, 28], which is required for the field-induced percolation. The electric field, in our case, is significantly weaker than that required for such transitions even at 100 V. The observed decrease in the conductance of the PEDOT : PSS + AuNP film at voltages above 50 V and during the subsequent scannings can be caused, in our opinion, by the accumulated space charge, which is hard to

withdraw in a weak electric field and at a low conductance.

The temperature dependence of the electrical conductance was determined at a fixed voltage of 10 V. Such dependences usually contain regions corresponding to the conductance of the material and the conductance of adsorbed oxygen [24, 25]. The electrical measurements of the pure PEDOT : PSS films demonstrated that atmospheric oxygen insignificantly affects their electrophysical properties. Figure 6a shows the temperature dependence of the conductance of the PEDOT : PSS films measured in the temperature range of 350–400 K. The linear character of this dependence, in combination with the lack of significant influence of adsorbed oxygen, allows us to conclude that the electrical conduction of the PEDOT films is provided only by intrinsic electron states with the conduction activation energy $E_a = 0.16$ eV calculated using the above relationship, and the hopping conduction activation energy can be represented as $E_{a1} = 0.99e^2n^{1/3}/4\pi\varepsilon_0\varepsilon$ [30], where e is the electron
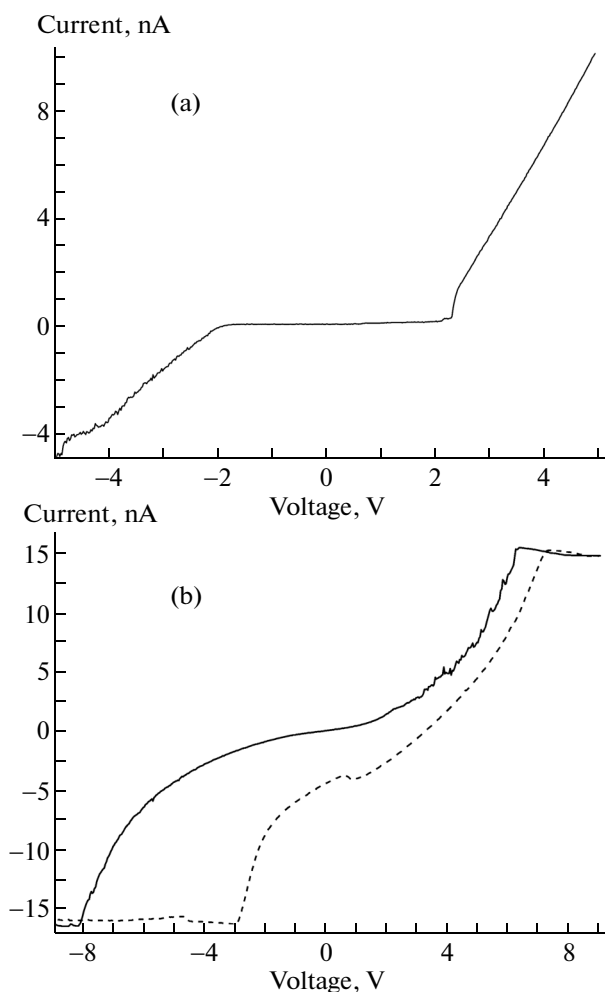
Fig. 4. Current–voltage characteristics of the film measured with a conductive atomic force microscope: (a) pure PEDOT : PSS and (b) PEDOT : PSS + AgNP. The solid and dashed lines correspond to the forward and reverse scanning modes, respectively.

charge, n is the concentration of localization centers, ε is the static relative permittivity of the material, and ε_0 is the dielectric constant.

A different situation occurs with the PEDOT : PSS + AuNP films. As can be seen from Fig. 6b, the temperature dependence of the conductance measured in the temperature range of 350–400 K is characterized by a deviation from linearity in the "logarithm of conductance–inverse temperature" coordinates. Usually, the deviation from linearity for disordered materials is associated with the mechanism of variable-range hopping conduction; in this case, the temperature dependence of the conductivity is described by the Mott law [31]: $\sigma = \sigma_0 \exp[-(T_0/T)^{1/4}]$. However, upon linearization of the experimental data obtained for the PEDOT: PSS + AuNP nanocomposite films in the $\ln G - (1/T)^n$ coordinates with an increase in the exponent n from 0.1 to 1.0, the linear correlation coeffi-
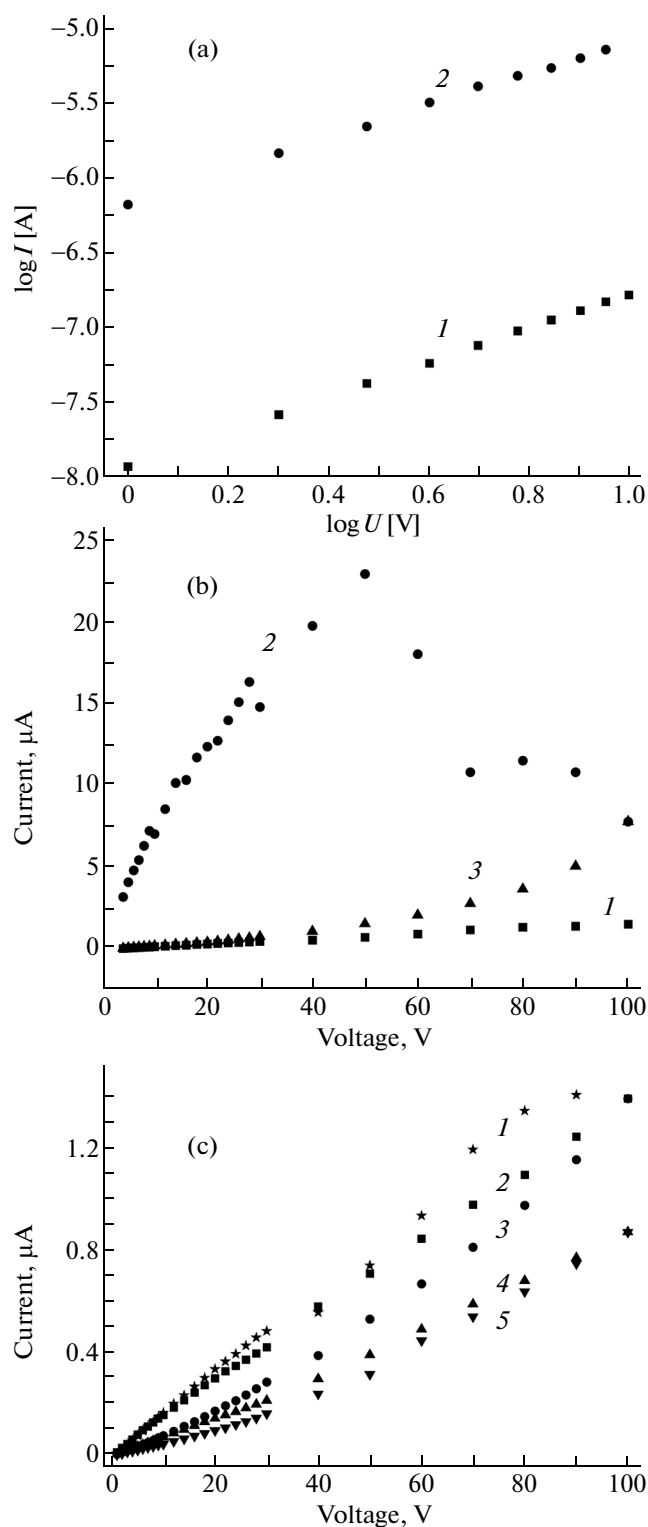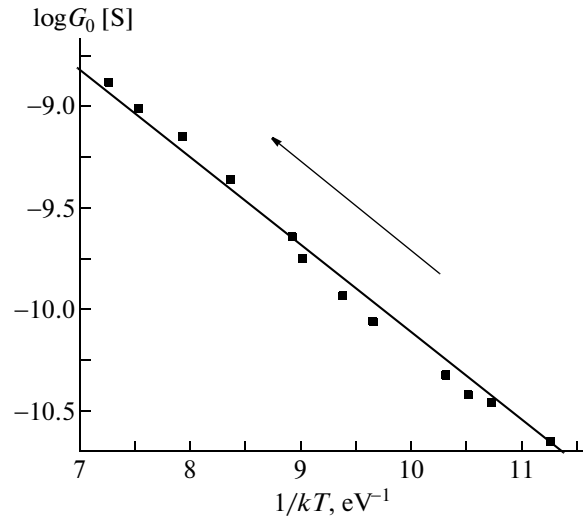

Fig. 5. Current–voltage characteristics of (*1*) pure PEDOT : PSS and (*2–5*) PEDOT : PSS + AuNP thin films on a substrate with interdigitated electrodes in the ranges (a) 0–10 and (b) 0–100 V for the first scanning and (c) 0–100 V for (*2*, *3*) second and (*4*, *5*) third scanning in (*2*, *4*) forward and (*3*, *5*) reverse modes.
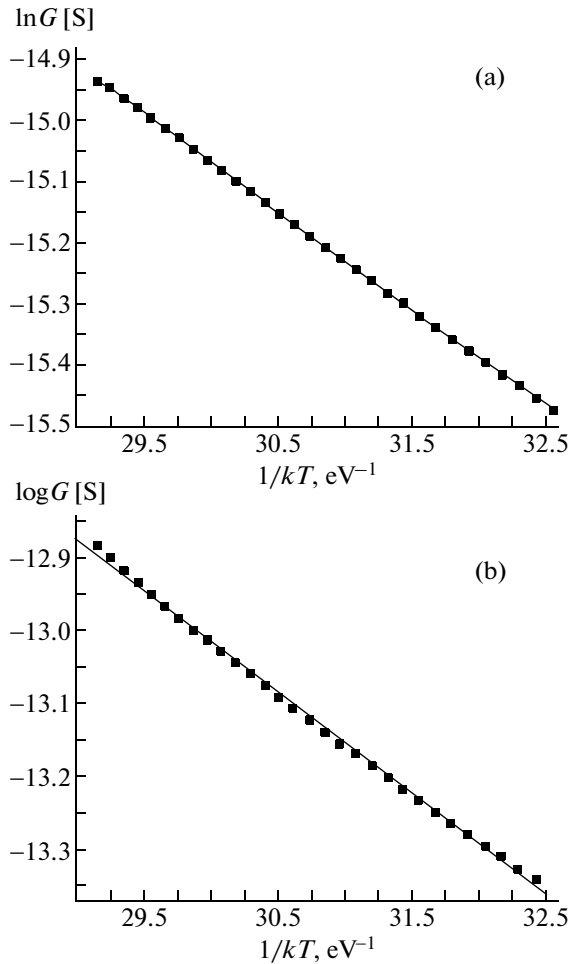
Fig. 6. Temperature dependences of the electrical conductance of the films measured in the temperature range of 350–400 K: (a) PEDOT : PSS and (b) PEDOT : PSS + AuNP.

Fig. 7. Correlation between the conduction activation energy and the pre-exponential factor in the expression describing the temperature dependence of the electrical conductance of the PEDOT : PSS + AuNP composite. The arrow indicates the direction of heating.

cient decreases monotonically from 0.9992 to 0.9983; i.e., there is no exact correspondence between the experimental data and the Mott law. Thus, we cannot reasonably argue that the temperature dependences of the conductivity of the PEDOT : PSS + AuNP nanocomposite are described by the expression of the form $\sigma = \sigma_0 \exp[-(T_0/T)^n]$.

At the same time, this nonlinearity can be due to the fact that the contribution to the conduction comes from both intrinsic electron states and states of adsorbed oxygen. In this case, the observed activation energy $E_a = -\partial(\ln G)/\partial(1/kT)$ is expressed as $E_a = (E_{a1}\sigma_1 + E_{a2}\sigma_2)/(\sigma_1 + \sigma_2)$ [24, 25], where E_{a1} and E_{a2} are the activation energies of the intrinsic conduction and impurity conduction, respectively; and σ_1 and σ_2 are the conductivities caused by intrinsic and impurity electron states, respectively. This hypothesis is consistent with the correlation between the conduction activation energy and the pre-exponential factor (Fig. 7) in the expression describing the temperature depen-

dence of the conductance measured for the PEDOT : PSS + AuNP films, where the maximum value of the conduction activation energy corresponds to the maximum temperature of the onset of cooling. This curve shows that the decrease in the concentration of adsorbed oxygen increases the concentration of localization centers providing electron transport. Therefore, the data presented in Figs. 5b and 6 indicate that the conduction of the PEDOT : PSS + AuNP films is provided by electron transfer over the common system of intrinsic states and states of adsorbed oxygen, with the dominant role played by impurity states.

4. CONCLUSIONS

It was found that the introduction of gold nanoparticles into PEDOT : PSS in weak electric fields leads to an increase in the bulk conductance by almost two orders of magnitude, a 50% decrease in the conduction activation energy, and an increase in the sensitivity to adsorbed oxygen. It was shown that electrical conduction of PEDOT : PSS + AuNP films is provided by hopping charge transfer both in the system of intrinsic localized states and in the system of impurity states of adsorbed oxygen rather than by variable-range hopping conduction. Gold nanoparticles promote the electron transfer due to donor–acceptor interactions in the nanocomposite. In stronger electric fields, an irreversible decrease in the electric current is observed after the first scanning. Possibly, this is associated with the accumulated space charge. The conductive atomic force microscopy measurements in strong electric fields revealed a nonlinear variation in the current and a different behavior of the current–voltage curves in the forward and reverse scanning

modes due to the electrically induced transitions with charge transfer from the donor moieties of the polymer to the metal acceptor. A more detailed explanation requires further investigation. The nanocomposite films obtained in this work remain transparent over the entire visible spectral range from 400 to 700 nm and retain their properties over a year under normal conditions.

ACKNOWLEDGMENTS

REFERENCES

1. H. S. Nalwa, *Handbook of Organic Electronics and Photonics* (American Scientific, Los Angeles, United States, 2008).

2. J. C. Scott and L. D. Bozano, Adv. Mater. (Weinheim) **19**, 1452 (2007).

3. T. W. Kim, Y. Yang, F. Li, and W. L. Kwan, NPG Asia Mater. **4**, e18 (2012).

4. Y. S. Hsiao, W. T. Whang, C. P. Chen, and Y. C. Chen, J. Mater. Chem. **18**, 5948 (2008).

5. C. C. D. Wang, W. C. H. Choy, C. Duan, D. D. S. Fung, W. E. I. Sha, F.-X. Xie, F. Huang, and Y. Cao, J. Mater. Chem. **22**, 1206 (2012).

6. A. D. Pomogailo, A. S. Rozenberg, and I. E. Uflyand, *Nanoparticles of Metals in Polymers* (Khimiya, Moscow, 2000) [in Russian].

7. C. C. Oey, A. B. Djurisic, S. Y. Kwong, C. H. Cheung, W. K. Chan, J. M. Nunzi, and P. C. Chui, Thin Solid Films **492**, 253 (2005).

8. F. Terzi, C. Zanardi, V. Martina, L. Pigani, and R. Seeber, J. Electroanal. Chem. **75**, 619 (2008).

9. A. V. Kukhta, E. E. Kolesnik, D. V. Ritchik, A. I. Lesnikovich, M. N. Nichick, and S. A. Vorobyova, in *Physics, Chemistry and Application of Nanostructures*, Ed. by V. E. Borisenko, S. V. Gaponenko, and V. S. Gurin (World Scientific, Singapore, 2005), p. 96.

10. C.-H. Lai, I-C. Wu, C.-C. Kang, J.-F. Lee, M.-L. Ho, and P.-T. Chou, Chem. Commun. (Cambridge) **2009**, 1996 (2009).

11. D. Hodko, M. Gamboa-Aldeco, and O. Murphy, J. Solid State Electrochem. **13**, 1063 (2009).

12. R. G. Melendez, K. J. Moreno, I. Moggio, E. Arias, A. Ponce, I. Llanera, and S. E. Moya, Mater. Sci. Forum **644**, 85 (2010).

13. C.-Y. Lee, Y.-J. Choi, S. Yoon, and H.-H. Park, Synth. Met. **160**, 621 (2010).

14. O. M. Folarin, E. R. Sadiku, and A. Maity, J. Phys. Sci. **6**, 4869 (2011).

15. J. Mathiyarasu, S. Senthilkumar, K. L. N. Phani, and V. Yegnaraman, J. Nanosci. Nanotechnol. **7**, 2206 (2007).

16. L. Groenendaal, F. Jonas, D. Freitag, H. Pielartzik, and J. R. Reynolds, Adv. Mater. (Weinheim) **12**, 481 (2000).

17. T. A. Skotheim and J. R. Reynolds, *Conjugated Polymers: Processing and Applications* (CRC Press, Boca Raton, Florida, United States, 2006).

18. B. D. Chin, J. Phys. D: Appl. Phys. **41**, 215104 (2008).

19. M. C. Scharber, D. Muhlbacher, M. Koppe, P. Denk, C. Waldauf, A. J. Heeger, and C. J. Brabec, Adv. Mater. (Weinheim) **18**, 789 (2006).

20. L. A. A. Pettersson, S. Ghosh, and O. Inganas, Org. Electron. **3**, 143 (2002).

21. S. Ghosh and O. Inganas, Synth. Met. **121**, 1321 (2001).

22. I. A. Milevich, S. A. Vorobyova, and A. I. Lesnikovich, Vestn. Belarus. Gos. Univ., Ser. 2 **1**, 33 (2011).

23. W. Wang, Sh. Efrima, and O. Regev, Langmuir **14**, 602 (1998).

24. A. E. Pochtenny and A. V. Misevich, Tech. Phys. Lett. **29** (1), 26 (2003).

25. A. V. Kukhto, E. E. Kolesnik, A. Lappo, A. E. Pochtenny, and I. K. Grabchev, Phys. Solid State **46** (12), 2306 (2004).

26. E. Hao and G. C. Schatz, J. Chem. Phys. **120**, 357 (2004).

27. L. D. Bozano, B. W. Kean, M. Beinhoff, K. R. Carter, P. M. Rice, and J. C. Scott, Adv. Funct. Mater. **15**, 1933 (2005).

28. Y. Yang, J. Ouyang, L. Ma, R. J.-H. Tseng, and C.-W. Chu, Adv. Funct. Mater. **16**, 1001 (2006).

29. J. Wu, L. Ma, and Y. Yang, Phys. Rev. B: Condens. Matter **69**, 15 321 (2004).

30. B. I. Shklovskii and A. L. Efros, *Electronic Properties of Doped Semiconductors* (Nauka, Moscow, 1979; Springer-Verlag, Berlin, 1984).

31. N. F. Mott and E. A. Davis, *Electron Processes in Noncrystalline Materials* (Clarendon, London, 1979).

Translated by O. Borovik-Romanova